NCSP
NUCLEAR CRITICALITY
SAFETY PROGRAM

LLNL-PRES-651897

Three COG Analytic Benchmarks

Presented at the Nuclear Criticality Safety Program (NCSP) Technical Program Review
March 26-27, 2014 at Los Alamos National Laboratory

Dave Heinrichs
Lawrence Livermore National Laboratory

Lawrence Livermore National Laboratory, P.O. Box 808, L-198, Livermore, CA 94551-0808
This work performed under the auspices of the U.S. Department of Energy by Lawrence Livermore National Laboratory under Contract DE-AC52-07NA27344

COG V&V Benchmarks

- Regression test suite (11 cases)
- ICSBEP (criticality) benchmarks (501 cases)
- SINBAD (shielding) benchmarks (9 cases)
- SILENE (CAAS/activation) benchmarks (11 cases)
- Photonuclear benchmarks (62 cases)
- NRF test suite (3 cases)
- Analytic benchmarks (**new and the subject of this presentation**)

V&V is a required element of SQA for 10CFR830 safety software

Three New Analytic Benchmarks – in COG

Kobayahsi

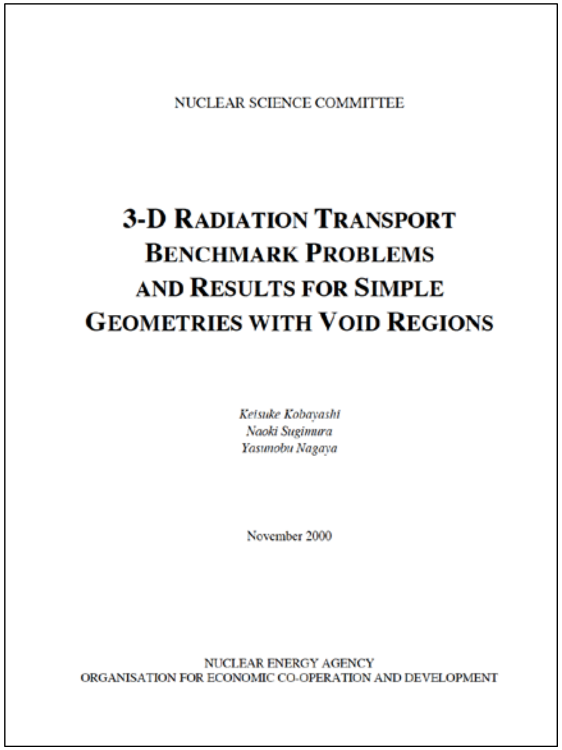

NUCLEAR SCIENCE COMMITTEE

3-D RADIATION TRANSPORT BENCHMARK PROBLEMS AND RESULTS FOR SIMPLE GEOMETRIES WITH VOID REGIONS

Keisuke Kobayashi
Naoki Sugimura
Yasunobu Nagaya

November 2000

NUCLEAR ENERGY AGENCY
ORGANISATION FOR ECONOMIC CO-OPERATION AND DEVELOPMENT

NSC-DOC2000-4 (2000)

Cylinder

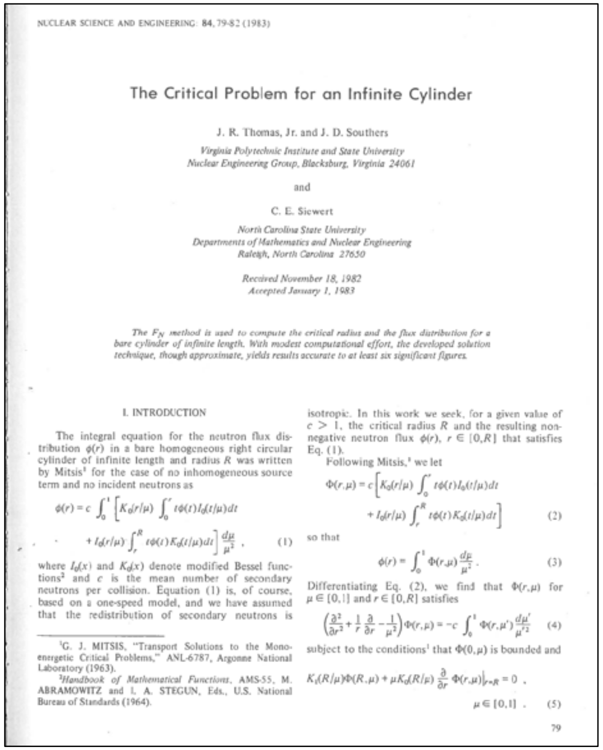

NUCLEAR SCIENCE AND ENGINEERING: **84**, 79-82 (1983)

The Critical Problem for an Infinite Cylinder

J. R. Thomas, Jr. and J. D. Southers
Virginia Polytechnic Institute and State University
Nuclear Engineering Group, Blacksburg, Virginia 24061

and

C. E. Siewert
North Carolina State University
Departments of Mathematics and Nuclear Engineering
Raleigh, North Carolina 27650

Received November 18, 1982
Accepted January 1, 1983

The F_N method is used to compute the critical radius and the flux distribution for a bare cylinder of infinite length. With modest computational effort, the developed solution technique, though approximate, yields results accurate to at least six significant figures.

I. INTRODUCTION

The integral equation for the neutron flux distribution $\phi(r)$ in a bare homogeneous right circular cylinder of infinite length and radius R was written by Mitsis[1] for the case of no inhomogeneous source term and no incident neutrons as

$$\phi(r) = c \int_0^1 \left[K_0(r/\mu) \int_0^r t\phi(t) I_0(t/\mu) dt + I_0(r/\mu) \int_r^R t\phi(t) K_0(t/\mu) dt \right] \frac{d\mu}{\mu^2} , \quad (1)$$

where $I_0(x)$ and $K_0(x)$ denote modified Bessel functions[2] and c is the mean number of secondary neutrons per collision. Equation (1) is, of course, based on a one-speed model, and we have assumed that the redistribution of secondary neutrons is isotropic. In this work we seek, for a given value of $c > 1$, the critical radius R and the resulting nonnegative neutron flux $\phi(r)$, $r \in [0,R]$ that satisfies Eq. (1).

Following Mitsis,[1] we let

$$\Phi(r,\mu) = c \left[K_0(r/\mu) \int_0^r t\phi(t) I_0(t/\mu) dt + I_0(r/\mu) \int_r^R t\phi(t) K_0(t/\mu) dt \right] \quad (2)$$

so that

$$\phi(r) = \int_0^1 \Phi(r,\mu) \frac{d\mu}{\mu^2} . \quad (3)$$

Differentiating Eq. (2), we find that $\Phi(r,\mu)$ for $\mu \in [0,1]$ and $r \in [0,R]$ satisfies

$$\left(\frac{\partial^2}{\partial r^2} + \frac{1}{r}\frac{\partial}{\partial r} - \frac{1}{\mu^2} \right) \Phi(r,\mu) = -c \int_0^1 \Phi(r,\mu') \frac{d\mu'}{\mu'^2} \quad (4)$$

subject to the conditions[1] that $\Phi(0,\mu)$ is bounded and

$$K_1(R/\mu)\Phi(R,\mu) + \mu K_0(R/\mu) \frac{\partial}{\partial r} \Phi(r,\mu)\Big|_{r=R} = 0 , \quad \mu \in [0,1] . \quad (5)$$

[1]G. J. MITSIS, "Transport Solutions to the Monoenergetic Critical Problems," ANL-6787, Argonne National Laboratory (1963).

[2]*Handbook of Mathematical Functions*, AMS-55, M. ABRAMOWITZ and I. A. STEGUN, Eds., U.S. National Bureau of Standards (1964).

79

NSE **84** 79-82 (1983)

Shmakov

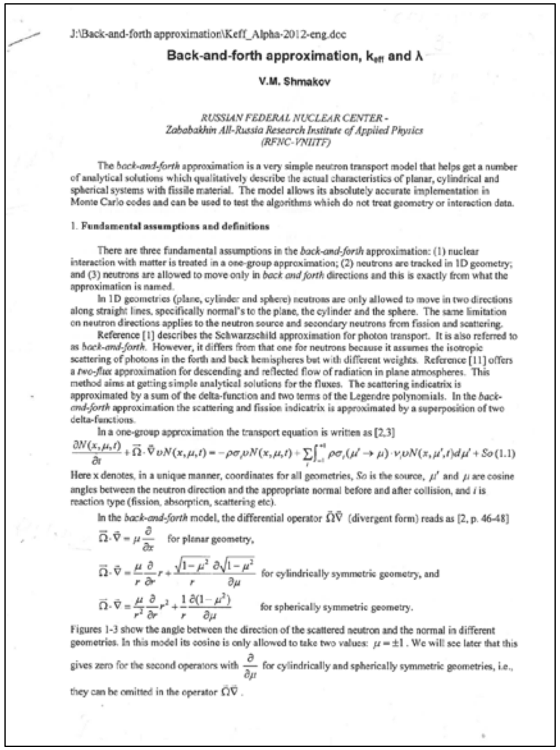

J:\Back-and-forth approximation\Keff_Alpha-2012-eng.doc

Back-and-forth approximation, k_{eff} and λ

V.M. Shmakov

RUSSIAN FEDERAL NUCLEAR CENTER -
Zababakhin All-Russia Research Institute of Applied Physics
(RFNC-VNIITF)

The *back-and-forth* approximation is a very simple neutron transport model that helps get a number of analytical solutions which qualitatively describe the actual characteristics of planar, cylindrical and spherical systems with fissile material. The model allows its absolutely accurate implementation in Monte Carlo codes and can be used to test the algorithms which do not treat geometry or interaction data.

1. **Fundamental assumptions and definitions**

There are three fundamental assumptions in the *back-and-forth* approximation: (1) nuclear interaction with matter is treated in a one-group approximation; (2) neutrons are tracked in 1D geometry; and (3) neutrons are allowed to move only in *back and forth* directions and this is exactly from what the approximation is named.

In 1D geometries (plane, cylinder and sphere) neutrons are only allowed to move in two directions along straight lines, specifically normal's to the plane, the cylinder and the sphere. The same limitation on neutron directions applies to the neutron source and secondary neutrons from fission and scattering.

Reference [1] describes the Schwarzschild approximation for photon transport. It is also referred to as *back-and-forth*. However, it differs from that one for neutrons because it assumes the isotropic scattering of photons in the forth and back hemispheres but with different weights. Reference [11] offers a *two-flux* approximation for descending and reflected flow of radiation in plane atmospheres. This method aims at getting simple analytical solutions for the fluxes. The scattering indicatrix is approximated by a sum of the delta-function and two terms of the Legendre polynomials. In the *back-and-forth* approximation the scattering and fission indicatrix is approximated by a superposition of two delta-functions.

In a one-group approximation the transport equation is written as [2,3]

$$\frac{\partial N(x,\mu,t)}{\partial t} + \vec{\Omega}\cdot\vec{\nabla}\upsilon N(x,\mu,t) = -\rho\sigma_t\upsilon N(x,\mu,t) + \sum_i \int_{-1}^{+1} \rho\sigma_i(\mu' \to \mu)\cdot \nu_i \upsilon N(x,\mu',t) d\mu' + So \quad (1.1)$$

Here x denotes, in a unique manner, coordinates for all geometries, So is the source, μ' and μ are cosine angles between the neutron direction and the appropriate normal before and after collision, and i is reaction type (fission, absorption, scattering etc).

In the *back-and-forth* model, the differential operator $\vec{\Omega}\vec{\nabla}$ (divergent form) reads as [2, p. 46-48]

$\vec{\Omega}\cdot\vec{\nabla} = \mu\frac{\partial}{\partial x}$ for planar geometry,

$\vec{\Omega}\cdot\vec{\nabla} = \frac{\mu}{r}\frac{\partial}{\partial r}r + \frac{\sqrt{1-\mu^2}}{r}\frac{\partial\sqrt{1-\mu^2}}{\partial\mu}$ for cylindrically symmetric geometry, and

$\vec{\Omega}\cdot\vec{\nabla} = \frac{\mu}{r^2}\frac{\partial}{\partial r}r^2 + \frac{1}{r}\frac{\partial(1-\mu^2)}{\partial\mu}$ for spherically symmetric geometry.

Figures 1-3 show the angle between the direction of the scattered neutron and the normal in different geometries. In this model its cosine is only allowed to take two values: $\mu = \pm 1$. We will see later that this gives zero for the second operators with $\frac{\partial}{\partial\mu}$ for cylindrically and spherically symmetric geometries, i.e., they can be omitted in the operator $\vec{\Omega}\vec{\nabla}$.

Unpublished manuscript (2012)

COG results published by Ed Lent as LLNL-TR-648225, Three Analytic Benchmarks in COG.

Kobayashi benchmarks – 3 problems

Problem 1

Figure 2. Sketch of Problem 1, shield with square void

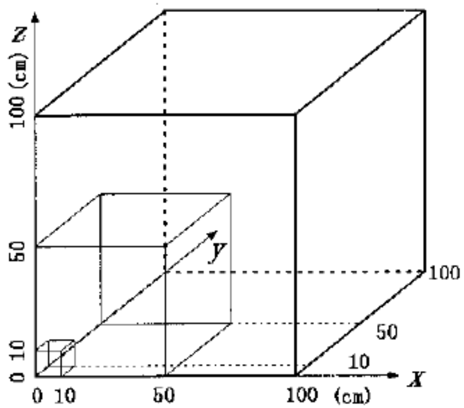

For all problems:

Region	S (n cm^{-3}s^{-1})	Σ_t (cm^{-1})
1	1	0.1
2	0	10^{-4}
3	0	0.1

Problem 2

Figure 4. Sketch of Problem 2, shield with void duct

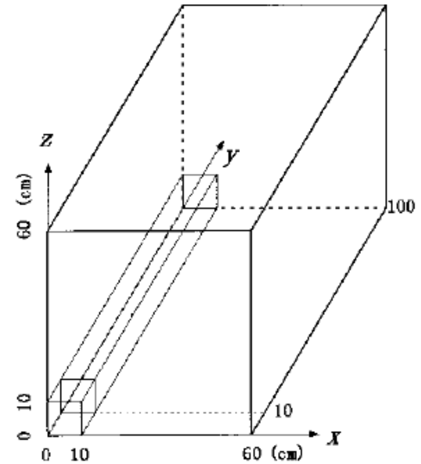

Problem 3

Figure 8. Sketch of Problem 3, shield with dog leg void duct

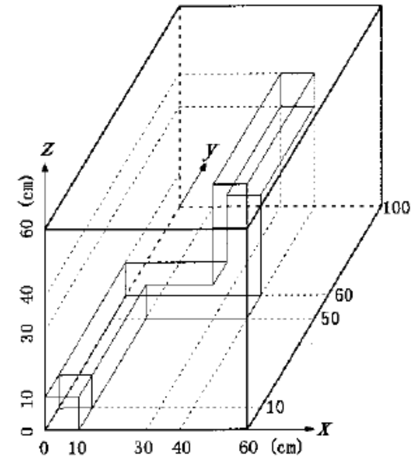

For pure absorbers (Σ_t=Σ_a), “exact” flux in the shield and duct are obtained by numerical integration:

$$\phi(\boldsymbol{r}) = \frac{1}{4\pi}\int_{V_s} d\boldsymbol{r}' \frac{\exp\left(-\int \Sigma_a(\boldsymbol{r}'')d\boldsymbol{r}''\right)S(\boldsymbol{r}')}{|\boldsymbol{r}-\boldsymbol{r}'|^2}$$

Kobayashi problem 1 results – φ

1A (x=z=5)

x,y,z	Analytic	COG	COG/Analytic
5,5,5	5.95659E+0	5.9537E+0 ± 1.48E-2	0.99952 ± 0.00250
5,15,5	1.37185E+0	1.3718E+0 ± 6.74E-5	0.99996 ± 0.00005
5,25,5	5.00871E-1	5.0086E-1 ± 1.55E-5	0.99998 ± 0.00003
5,35,5	2.52429E-1	2.5242E-1 ± 6.66E-6	0.99996 ± 0.00003
5,45,5	1.50260E-1	1.5026E-1 ± 3.64E-6	1.00000 ± 0.00002
5,55,5	5.95286E-2	5.9530E-2 ± 1.36E-6	1.00002 ± 0.00002
5,65,5	1.53283E-2	1.5328E-2 ± 3.34E-7	0.99998 ± 0.00002
5,75,5	4.17689E-3	4.1769E-3 ± 8.85E-8	1.00000 ± 0.00002
5,85,5	1.18533E-3	1.1854E-3 ± 2.44E-8	1.00006 ± 0.00002
5,95,5	3.46846E-4	3.4686E-4 ± 7.01E-9	1.00004 ± 0.00002

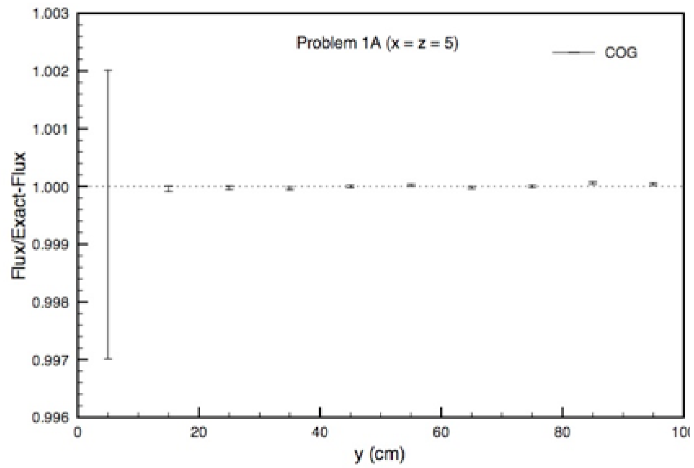

Figure 2. Sketch of Problem 1, shield with square void

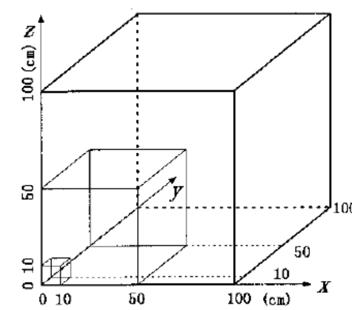

1B (x=y=z)

x,y,z	Analytic	COG	COG/Analytic
5,5,5	5.95659E+0	5.9537E+0 ± 1.49E-2	0.99952 ± 0.00250
15,15,15	4.70754E-1	4.7083E-1 ± 5.84E-5	1.00016 ± 0.00012
25,25,25	1.69968E-1	1.6998E-1 ± 1.36E-5	1.00007 ± 0.00008
35,35,35	8.68334E-2	8.6838E-2 ± 6.05E-6	1.00005 ± 0.00007
45,45,45	5.25132E-2	5.2515E-2 ± 3.41E-6	1.00003 ± 0.00007
55,55,55	1.33378E-2	1.3338E-2 ± 8.27E-7	1.00001 ± 0.00006
65,65,65	1.45867E-3	1.4587E-3 ± 8.83E-8	1.00002 ± 0.00006
75,75,75	1.75364E-4	1.7537E-4 ± 1.05E-8	1.00003 ± 0.00006
85,85,85	2.24607E-5	2.2462E-5 ± 1.34E-9	1.00006 ± 0.00006
95,95,95	3.01032E-6	3.0105E-6 ± 1.8E-10	1.00006 ± 0.00006

1C (y=55, z=5)

x,y,z	Analytic	COG	COG/Analytic
5,55,5	5.95290E-2	5.9530E-2 ± 4.50E-6	1.00000 ± 0.00008
15,55,5	5.50250E-2	5.5026E-2 ± 4.09E-6	1.00000 ± 0.00007
25,55,5	4.80750E-2	4.8077E-2 ± 3.47E-6	1.00000 ± 0.00007
35,55,5	3.96770E-2	3.9677E-2 ± 2.80E-6	1.00000 ± 0.00007
45,55,5	3.16370E-2	3.1637E-2 ± 2.19E-6	1.00000 ± 0.00007
55,55,5	2.35300E-2	2.3530E-2 ± 1.59E-6	0.99999 ± 0.00007
65,55,5	5.83720E-3	5.8372E-3 ± 3.98E-7	1.00000 ± 0.00007
75,55,5	1.56730E-3	1.5673E-3 ± 1.06E-7	0.99999 ± 0.00007
85,55,5	4.53110E-4	4.5311E-4 ± 3.04E-8	0.99999 ± 0.00007
95,55,5	1.37080E-4	1.3708E-4 ± 9.10E-9	1.00000 ± 0.00007

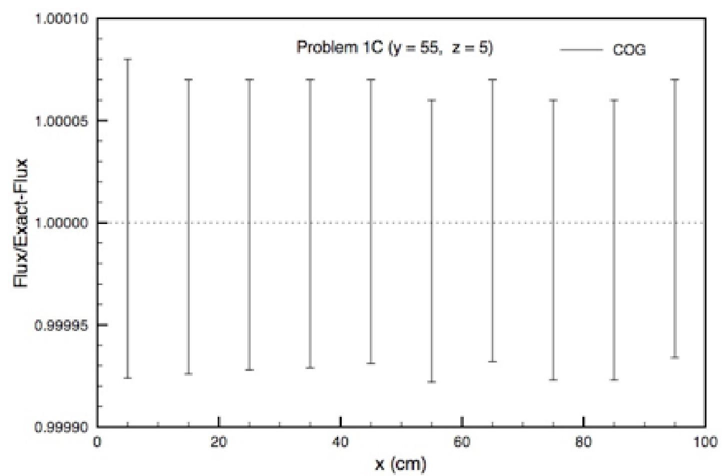

The results for Problem 1 are EXCELLENT; 24 (86%) ≤ 1σ; 3 (11%) ≤ 2σ; 1 (4%) ≤ 3σ

Kobayashi problem 2 results – φ

2A (x=z=5)

x,y,z	Analytic	COG	COG/Analytic
5,5,5	5.95659E+0	5.9510E+0 ± 1.57E-2	0.99900 ± 0.00263
5,15,5	1.37185E+0	1.3717E+0 ± 2.24E-4	0.99989 ± 0.00016
5,25,5	5.00871E-1	5.0088E-1 ± 5.11E-5	1.00002 ± 0.00010
5,35,5	2.52429E-1	2.5244E-1 ± 2.21E-5	1.00004 ± 0.00009
5,45,5	1.50260E-1	1.5027E-1 ± 1.21E-5	1.00007 ± 0.00008
5,55,5	9.91726E-2	9.9176E-2 ± 7.51E-6	1.00003 ± 0.00008
5,65,5	7.01791E-2	7.0182E-2 ± 5.10E-6	1.00004 ± 0.00007
5,75,5	5.22062E-2	5.2208E-2 ± 3.68E-6	1.00003 ± 0.00007
5,85,5	4.03188E-2	4.0320E-2 ± 2.77E-6	1.00003 ± 0.00007
5,95,5	3.20574E-2	3.2059E-2 ± 2.16E-6	1.00005 ± 0.00007

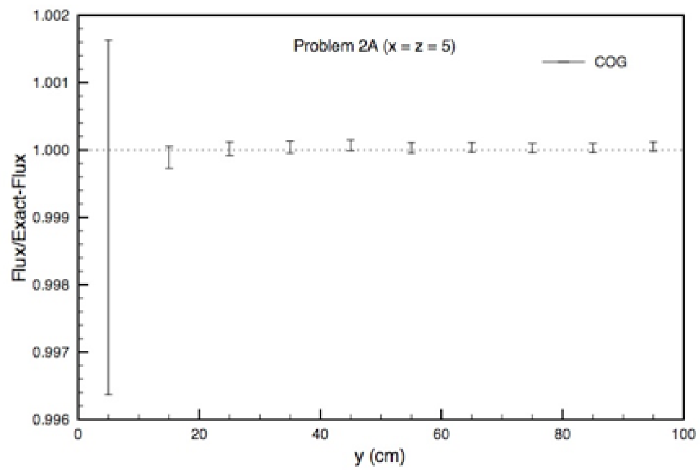

2B (y=95, z=5)

x,y,z	Analytic	COG	COG/Analytic
5,95,5	3.20574E-2	3.2058E-2 ± 2.16E-6	1.00002 ± 0.00007
15,95,5	1.70541E-3	1.7053E-3 ± 2.27E-7	0.99994 ± 0.00013
25,95,5	1.40557E-4	1.4055E-4 ± 2.09E-8	0.99995 ± 0.00015
35,95,5	3.27058E-5	3.2704E-5 ± 4.68E-9	0.99995 ± 0.00014
45,95,5	1.08505E-5	1.0851E-5 ± 1.44E-9	1.00000 ± 0.00013
55,95,5	4.14132E-6	4.1412E-6 ± 5.1E-10	0.99997 ± 0.00012

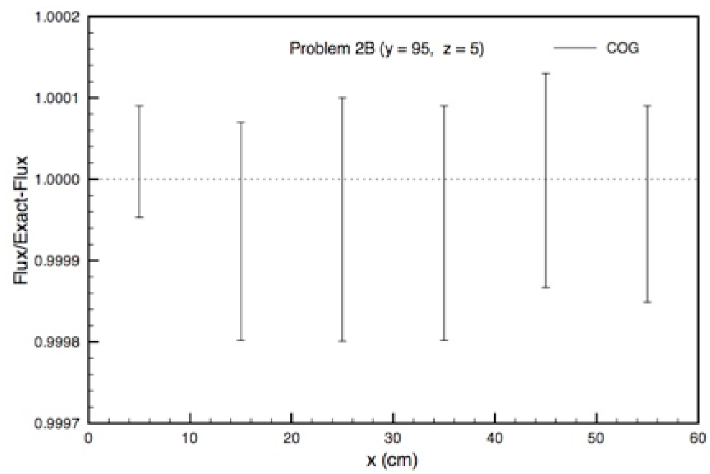

Figure 4. Sketch of Problem 2, shield with void duct

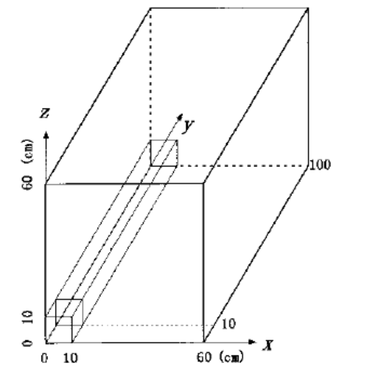

The results for Problem 2 are EXCELLENT; 15 (100%) ≤ 1σ; 0 (0%) ≤ 2σ; 0 (0%) ≤ 3σ

Kobayashi problem 3 results – φ

3A (x=z=5)

x,y,z	Analytic	COG	COG/Analytic
5,5,5	5.95659E+0	5.9524E+0 ± 8.93E-3	0.99930 ± 0.00150
5,15,5	1.37185E+0	1.3720E+0 ± 2.24E-4	1.00011 ± 0.00016
5,25,5	5.00871E-1	5.0093E-1 ± 5.11E-5	1.00012 ± 0.00010
5,35,5	2.52429E-1	2.5246E-1 ± 2.21E-5	1.00012 ± 0.00009
5,45,5	1.50260E-1	1.5028E-1 ± 1.21E-5	1.00013 ± 0.00008
5,55,5	9.91726E-2	9.9185E-2 ± 7.51E-6	1.00013 ± 0.00008
5,65,5	4.22623E-2	4.2267E-2 ± 3.06E-6	1.00011 ± 0.00007
5,75,5	1.14703E-2	1.1472E-2 ± 8.05E-7	1.00015 ± 0.00007
5,85,5	3.24662E-3	3.2470E-3 ± 2.22E-7	1.00012 ± 0.00007
5,95,5	9.48324E-4	9.4844E-4 ± 6.36E-8	1.00012 ± 0.00007

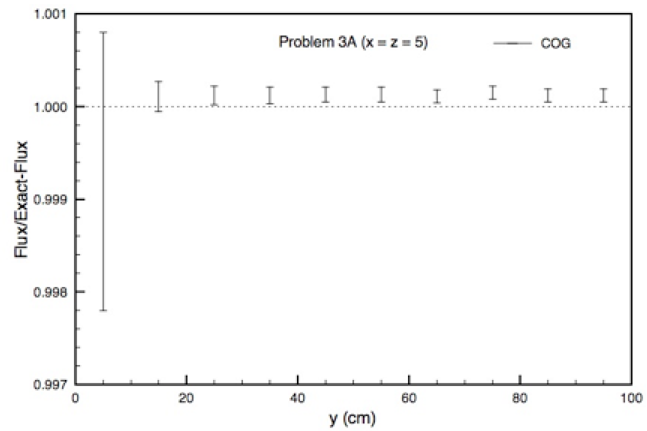

3B (y=55, z=5)

x,y,z	Analytic	COG	COG/Analytic
5,55,5	9.91726E-2	9.9172E-2 ± 7.51E-6	0.99999 ± 0.00008
15,55,5	2.45041E-2	2.4503E-2 ± 2.82E-6	0.99996 ± 0.00012
25,55,5	4.54477E-3	4.5445E-3 ± 5.45E-7	0.99994 ± 0.00012
35,55,5	1.42960E-3	1.4295E-3 ± 1.60E-7	0.99993 ± 0.00011
45,55,5	2.64846E-4	2.6483E-4 ± 2.70E-8	0.99994 ± 0.00010
55,55,5	9.14210E-5	9.1418E-5 ± 8.40E-9	0.99997 ± 0.00009

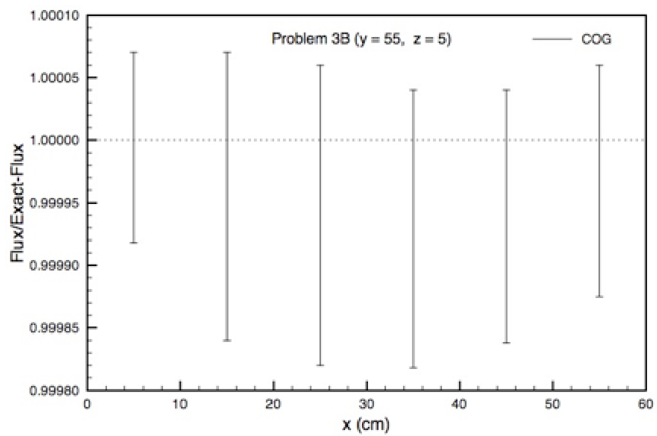

3C (y=95, z=35)

x,y,z	Analytic	COG	COG/Analytic
5,95,35	3.27058E-5	3.2701E-5 ± 4.68E-9	0.99985 ± 0.00014
15,95,35	2.68415E-5	2.6837E-5 ± 4.00E-9	0.99983 ± 0.00015
25,95,35	1.70019E-5	1.6999E-5 ± 2.70E-9	0.99983 ± 0.00016
35,95,35	3.37981E-5	3.3791E-5 ± 4.97E-9	0.99979 ± 0.00015
45,95,35	6.04893E-6	6.0480E-6 ± 8.2E-10	0.99985 ± 0.00014
55,95,35	3.36460E-6	3.3642E-6 ± 3.0E-10	0.99988 ± 0.00009

Figure 8. Sketch of Problem 3, shield with dog leg void duct

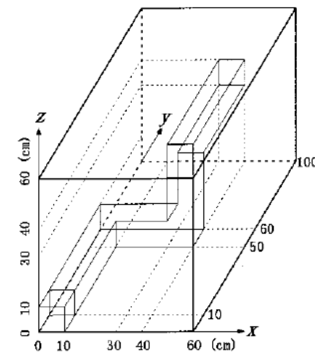

The results for Problem 3 are EXCELLENT; 8 (36%) ≤ 1σ; 14 (64%) ≤ 2σ; 0 (0%) ≤ 3σ

Cylinder benchmarks

TABLE 1

The Critical Radius in Mean-Free-Paths

c	F_N	Westfall (Ref. 6)	Sanchez (Ref. 10)
1.01	13.12551647		13.12551647
1.02	9.04325484	9.043255	
1.05	5.41128828	5.411288	
1.1	3.57739129	3.577391	3.57739129
1.2	2.28720926	2.287209	
1.3	1.72500292		1.72500292
1.4	1.39697859	1.396979	
1.5	1.17834084		1.17834085
1.6	1.02083901	1.020839	
1.8	0.80742662	0.807427	
2.0	0.66861286	0.668613	0.66861287

TABLE II

The Normalized Flux Distribution $\phi(r)/\phi(0)$

r/R	$c = 1.05$	$c = 1.1$	$c = 1.6$	$c = 2.0$
0	1	1	1	1
0.25	0.929851	0.936052	0.954996	0.959783
0.50	0.733990	0.756084	0.824845	0.842634
0.75	0.452168	0.492189	0.621823	0.656963
0.85	0.326662	0.371791	0.522344	0.564397
0.91	0.249166	0.296040	0.456627	0.502561
0.95	0.195805	0.243013	0.408837	0.457217
0.98	0.153085	0.199922	0.368807	0.418991
1	0.117908	0.164122	0.335065	0.386649

Critical radius and flux determined numerically using the F_N method to solve a singular integral equation using basis functions.

Cylinder benchmark results – R_C and φ

COG criticality calculations to search for the radius corresponding to $k_{eff} = 1$

Critical Radius

c	Thomas et al	COG	Ratio
1.01	13.12551647	13.129000	1.00027
1.02	9.04325484	9.071907	1.00317
1.05	5.41128828	5.406602	0.99913
1.1	3.57739129	3.576979	0.99988
1.2	2.28720926	2.287167	0.99998
1.3	1.72500292	1.724991	0.99999
1.4	1.39697859	1.396939	0.99997
1.5	1.17834084	1.178302	0.99997
1.6	1.02083901	1.020835	1.00000
1.8	0.80742662	0.807410	0.99998
2	0.66861286	0.668612	1.00000

Flux (c=1.05)

r/R	Thomas et al	COG	Ratio
0	1.000000	1.00450 ± 0.01552	1.00450 ± 0.01552
0.25	0.929851	0.93038 ± 0.00049	1.00060 ± 0.00053
0.5	0.733990	0.73366 ± 0.00031	0.99955 ± 0.00042
0.75	0.452168	0.45185 ± 0.00018	0.99929 ± 0.00039
0.85	0.326662	0.32666 ± 0.00015	1.00000 ± 0.00045
0.91	0.249166	0.24913 ± 0.00012	0.99987 ± 0.00047
0.95	0.195805	0.19581 ± 0.00010	1.00000 ± 0.00050
0.98	0.153085	0.15315 ± 0.00009	1.00040 ± 0.00056
1	0.117908	0.11800 ± 0.00005	1.00070 ± 0.00042

Flux (c=2)

r/R	Thomas et al	COG	Ratio
0	1.000000	0.98526 ± 0.03887	0.98526 ± 0.03887
0.25	0.959783	0.96013 ± 0.00046	1.00036 ± 0.00048
0.5	0.842634	0.84248 ± 0.00029	0.99981 ± 0.00034
0.75	0.656963	0.65718 ± 0.00019	1.00033 ± 0.00029
0.85	0.564397	0.56425 ± 0.00015	0.99974 ± 0.00027
0.91	0.502561	0.50261 ± 0.00013	1.00009 ± 0.00026
0.95	0.457217	0.45700 ± 0.00011	0.99953 ± 0.00024
0.98	0.418991	0.41896 ± 0.00009	0.99993 ± 0.00022
1	0.386649	0.38672 ± 0.00005	1.00017 ± 0.00014

The results for the cylinder benchmarks are EXCELLENT

Shmakov benchmarks – k_{eff}, λ and φ

- Shmakov solves the one-speed neutron transport equation to obtain simple closed-form analytical expressions for:
  - k_{eff} (criticality) or λ (alpha)
  - φ (and reaction rates)
- Solution is easy due to back-and-forth approximation (μ=±1)
- For example – a solid sphere:

$$\boxed{\rho R = \frac{\arctan\left(\sqrt{\frac{b+a}{b-a}}\right)}{\sqrt{b^2 - a^2}}}$$

$$\boxed{4\pi r^2 v N(r,\mu) = \frac{1}{2} u(0)\left\{\cos\left(\rho r\sqrt{b^2 - a^2}\right)\left[\delta(1-\mu) + \delta(1+\mu)\right] + \sqrt{\frac{b-a}{b+a}}\sin\left(\rho r\sqrt{b^2 - a^2}\right)\left[\delta(1-\mu) - \delta(1+\mu)\right]\right\}}$$

where $b + a = \sigma_t - \sigma_s(1 - 2q)$ and $b - a = \sigma_f\left(\frac{\nu}{k} - 1\right) - \sigma_c$

- Back-and-forth scattering model added to COG to enable comparison to exact analytic values

Shmakov benchmarks – solid sphere k_{eff} and λ

- One group parameters

σ_s	6.47 bn	scattering cross section
q	0.1	probability of back scatter for σ_s
σ_a	0.13 bn	absorption cross section
σ_f	1.25 bn	fission cross section
	0.5	probability of back scatter for σ_f
ν_f	2.6	neutrons per fission
E	1 MeV	neutron energy
v	138 cm/10^{-7} s	neutron velocity

- k_{eff} (criticality) and λ (λ = α/10, where α is in gen/μsec)

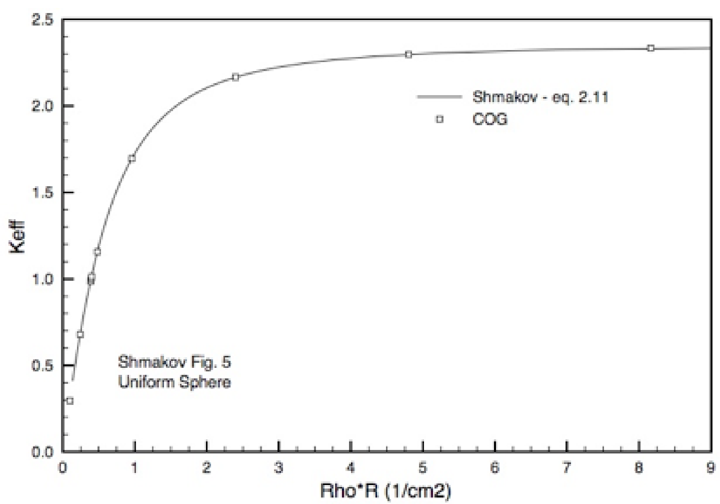

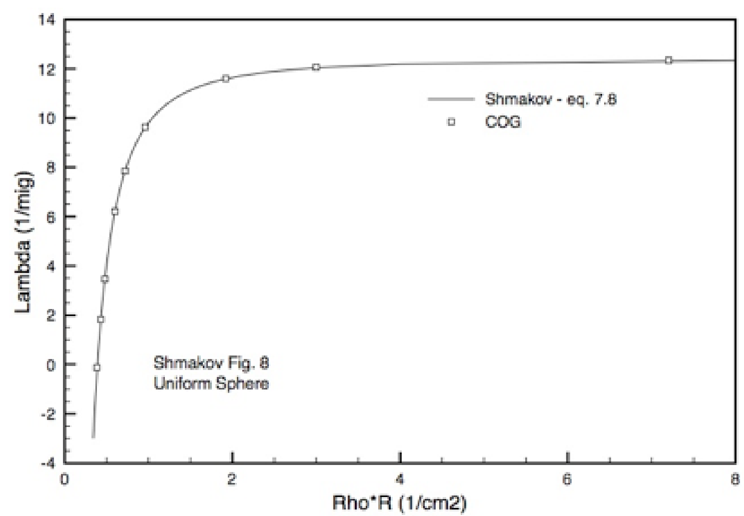

The results for the Shmakov solid sphere benchmarks are EXCELLENT

Shmakov benchmarks – hollow sphere k_{eff} and φ

- k_{eff} (criticality) and flux (U=outward, S=inward)

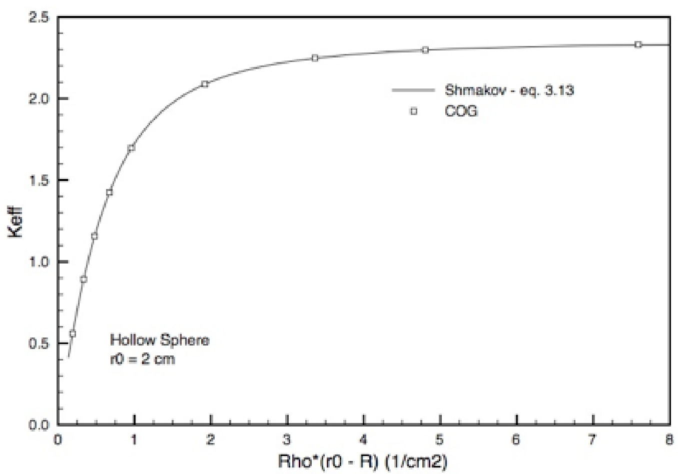

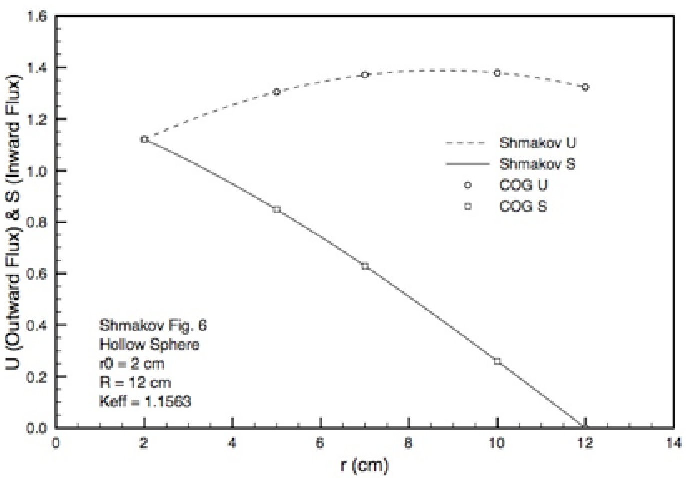

- Reaction rates (balance table) for r0=2 cm and R=12 cm

	Analytic	COG	COG/Analytic
Leakage	1.3234298	1.32335 ± 0.00009	0.99994 ± 0.00007
Scattered	5.9850792	5.98491 ± 0.00019	0.99996 ± 0.00003
Fissioned	1.1563136	1.15637 ± 0.00007	1.00005 ± 0.00006
Absorbed	0.1202566	0.12025 ± 0.00003	0.99995 ± 0.00025
Collided	7.2616495	7.26153 ± 0.00022	0.99998 ± 0.00003
ν_f	2.6	2.60002	1.00001
k_{eff}	1.1563136	1.15637 ± 0.00007	1.00005 ± 0.00006

The results for the Shmakov hollow sphere benchmarks are EXCELLENT

Conclusion

- COG performance is excellent
- No coding errors were discovered providing additional confidence in the algorithms in COG
- The Shmakov benchmarks are an excellent contribution to the field of analytical benchmarks
- Additional benchmarks are in progress in support of LLNL operations

Questions?

COG11.1 – New Features, Data, V&V

Rich Buck, Dave Heinrichs, Chuck Lee, Ed Lent
Lawrence Livermore National Laboratory, 7000 East Avenue, L-198, Livermore, CA, 94550, USA
This work performed under the auspices of the U.S. Department of Energy by Lawrence Livermore National Laboratory under Contract DE-AC52-07NA27344.

Paris - 2013

New Features

CritDetVR – Enables hybrid criticality/shielding calculations for variance reduction of detector scores with no bias in the keff calculation.
DFG – Simulates delayed gamma emission from the fission product decay.
NRF – Simulates nuclear resonance fluorescence reactions for nuclear photon absorption and emission.
RadSrc – Automatic photon source calculation for gamma emission from α-decay at a user-specified time (age).
COGLEX – Update includes dictionary entries for compounds with thermal scattering law.

New Data Libraries

NRF Library (Dr. Jim Hall, LLNL):
- COGNRF

RadSrc Library (Dr. Ed Lent, LLNL):
- COGRS

DFG Libraries (Dr. Ed Lent, LLNL):
- DFG.ENDFB7R1
- DFG.JEFF3.1.1
- DFG.JENDL4

Neutron Libraries:
- ENDFB7R1, PT.ENDFB7R1, T.ENDFB7R1
- JEFF3.1.2, PT.JEFF3.1.2, T.JEFF3.1.2
- JENDL4

Dosimetry Library:
- IRDFF1.02

Supported Library Formats:
- ENDL, ENDF, ACE
- GND (in progress)

Many, many older data libraries continue to be supported (e.g., JEF2.2, ENDF/B-V).

MC-to-S_N

ARDRA – COG geometry package is included in LLNL's modern massively parallel S_N code with automatic meshing features.

V&V

COG11BETA2 has been extensively tested using the following test suites:
- Regression tests (11 cases)
- ICSBEP criticality benchmarks (501 cases)
- NRF tests (3 cases)
- SINBAD shielding benchmarks (9 cases)
- SILENE Activation benchmarks (11 cases)
- PHOTONUCLEAR benchmarks (16)
- KOBAYASHI exact solutions (in progress)
- CRITCYL exact solutions (in progress)

Automation

LLNL is automating V&V code/data testing as described by M.-A. Descalle at ND2013. BNL is involved in a similar effot.

Website/Email

Please visit our website at http://cog.llnl.gov and contact us at COG@llnl.gov.

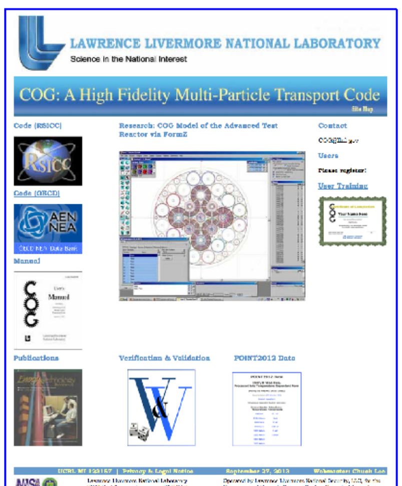

LLNL-POST-644394

COG11.1 – Practical Applications

Rich Buck, Dave Heinrichs, Chuck Lee, Ed Lent
Lawrence Livermore National Laboratory, 7000 East Avenue, L-198, Livermore, CA, 94550, USA
This work performed under the auspices of the U.S. Department of Energy by Lawrence Livermore National Laboratory under Contract DE-AC52-07NA27344.

Paris - 2013

SILENE Activation Experiment

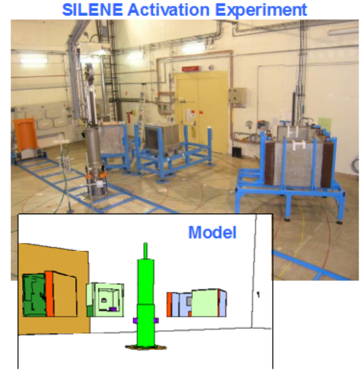

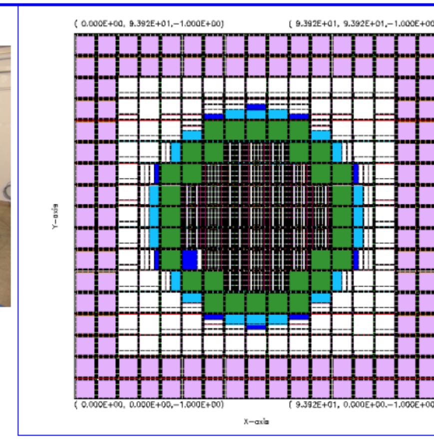

Detailed Model of ZPPR-21F
Reactor Physics

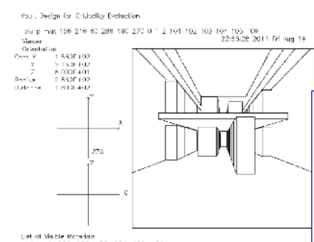

Storage Vault Model
Shielding & Criticality Safety

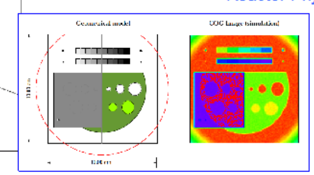

Neutron Radiography

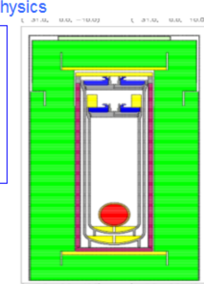

9975 Shipping Container
Shielding & Criticality

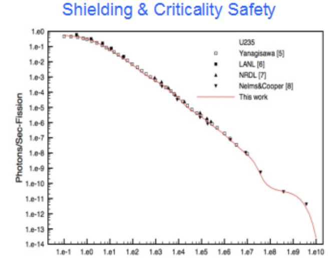

Fission Product Decay Gammas
Dose Assessment

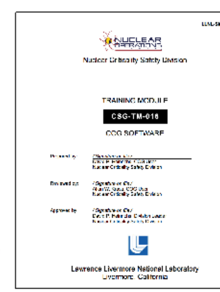

Practical User Training

LLNL-POST-644395